THE JOURNAL OF BIOLOGICAL CHEMISTRY
Vol. 279, No. 31, Issue of July 30, pp. 32515–32523, 2004
Printed in U.S.A.

Roles of Conserved P Domain Residues and Mg^{2+} in ATP Binding in the Ground and Ca^{2+}-activated States of Sarcoplasmic Reticulum Ca^{2+}-ATPase*

Received for publication, March 23, 2004, and in revised form, April 28, 2004
Published, JBC Papers in Press, May 7, 2004, DOI 10.1074/jbc.M403242200

David B. McIntosh‡§, Johannes D. Clausen¶, David G. Woolley‡, David H. MacLennan‖, Bente Vilsen¶, and Jens Peter Andersen¶**

From ‡Chemical Pathology, Department of Clinical Laboratory Sciences, Faculty of Health Sciences, University of Cape Town, and National Health Laboratory Service, Groote Schuur Hospital, Cape Town 7925, South Africa, the ‖Banting and Best Department of Medical Research, University of Toronto, Toronto, Ontario M5G 1L6, Canada, and the ¶Department of Physiology, University of Aarhus, DK-8000 Aarhus C, Denmark

Residues in conserved motifs ^{625}TGD, ^{676}FARXXPXXK, and ^{701}TGDGVND in domain P of sarcoplasmic reticulum Ca^{2+}-ATPase, as well as in motifs ^{601}DPPR and ^{359}NQR(/K)MSV in the hinge segments connecting domains N and P, were examined by mutagenesis to assess their roles in nucleotide and Mg^{2+} binding and stabilization of the Ca^{2+}-activated transition state for phosphoryl transfer. In the absence of Mg^{2+}, mutations removing the charges of domain P residues Asp^{627}, Lys^{684}, Asp^{703}, and Asp^{707} increased the affinity for ATP and 2′,3′-*O*-(2,4,6-trinitrophenyl)-8-azidoadenosine 5′-triphosphate. These mutations, as well as Gly^{626}→Ala, were inhibitory for ATP binding in the presence of Mg^{2+} and for tight binding of the β,γ-bidentate chromium(III) complex of ATP. The hinge mutations had pronounced, but variable, effects on ATP binding only in the presence of Mg^{2+}. The data demonstrate an unfavorable electrostatic environment for binding of negatively charged nucleotide in domain P and show that Mg^{2+} is required to anchor the phosphoryl group of ATP at the phosphorylation site. Mutants Gly^{626} → Ala, Lys^{684} → Met, Asp^{703} → Ala/Ser/Cys, and mutants with alteration to Asp^{707} exhibited very slow or negligible phosphorylation, making it possible to measure ATP binding in the pseudo-transition state attained in the presence of both Mg^{2+} and Ca^{2+}. Under these conditions, ATP binding was almost completely blocked in Gly^{626} → Ala and occurred with 12- and 7-fold reduced affinities in Asp^{703} → Ala and Asp^{707} → Cys, respectively, relative to the situation in the presence of Mg^{2+} without Ca^{2+}, whereas in Lys^{684} → Met and Asp^{707} → Ser/Asn the affinity was enhanced 14- and 3–5-fold, respectively. Hence, Gly^{626} and Asp^{703} seem particularly critical for mediating entry into the transition state for phosphoryl transfer upon Ca^{2+} binding at the transport sites.

The sarcoplasmic reticulum Ca^{2+}-ATPase[1] from rabbit muscle couples the hydrolysis of ATP to the transport of Ca^{2+} to the reticular lumen, and the lowering of the sarcoplasmic Ca^{2+} concentration leads to muscle relaxation. This ion pump is a well studied example of P-type ATPases, the catalytic cycle of which includes a phosphorylated aspartyl intermediate and progression through E1 and E2 states. ATP-dependent phosphorylation takes place upon Ca^{2+} binding in the E1 form, and hydrolysis of the aspartyl phosphoryl bond occurs in the E2P phosphoenzyme conformation following Ca^{2+} translocation across the membrane. Two atomic structures of the protein have been elucidated by x-ray crystallography, one in the presence of Ca^{2+} (designated E1(Ca_2)) and another in the absence of Ca^{2+} and presence of the specific inhibitor thapsigargin (E2(TG)) (1, 2). They reveal 10 membrane-spanning helices, connected through a stalk section to the phosphorylation (P) domain in association with nucleotide (N) and actuator (A) domains. The three head domains are loosely attached in E1(Ca_2) and closer together, forming a more compact entity, in E2(TG). For ATP-dependent phosphorylation of Asp^{351} to occur in the Ca^{2+} bound E1 state, domain N must close over the phosphorylation site, such that the nucleotide site is brought close to Asp^{351}. ATP likely straddles both domains, the nucleoside portion anchored in domain N and the phosphates stretching into domain P (*cf.* Fig. 1*A*).

Domain P contains the highly conserved segments ^{625}TGD, ^{676}FARXXPXXK, and ^{701}TGDGVND that surround the phosphorylation loop ^{351}DKTGTLT. Many of these residues have been implicated in ATP binding and catalysis on the basis of chemical labeling and cross-linking experiments, and mutagenesis of Ca^{2+}-ATPase and related pumps (for review, see Ref. 3). Most of them recur at the active site of a large class of soluble phosphohydrolases and phosphotransferases believed to have a similar reaction mechanism (4). Atomic structures of several intermediate or pseudo-intermediate states have pro-

* This work was supported in part by grants from the National Research Foundation of South Africa and University of Cape Town Research Committee (to D. B. M.), the Danish Medical Research Council, the Novo Nordisk Foundation, Denmark, the Lundbeck Foundation (Denmark), and the Research Foundation of Aarhus University (to J. P. A.), and by Canadian Institutes of Health Research Grant MT 12545 (to D. H. M.). The costs of publication of this article were defrayed in part by the payment of page charges. This article must therefore be hereby marked "*advertisement*" in accordance with 18 U.S.C. Section 1734 solely to indicate this fact.

§ To whom correspondence may be addressed: Chemical Pathology, Dept. of Clinical Laboratory Sciences, Faculty of Health Sciences, University of Cape Town, Cape Town 7925, South Africa. Fax: 27-21-4488150; E-mail: davidmci@chempath.uct.ac.za.

** To whom correspondence may be addressed: Dept. of Physiology, University of Aarhus, Ole Worms Allé 160, DK-8000 Aarhus C, Denmark. Fax: 45-86129065; E-mail: jpa@fi.au.dk.

[1] The abbreviations used are: Ca^{2+}-ATPase, the sarco(endo)plasmic reticulum Ca^{2+}-transporting adenosine triphosphatase (EC 3.6.1.38); CrATP, β,γ-bidentate chromium(III) complex of ATP; E1, enzyme form with cytoplasmically facing high affinity Ca^{2+} binding sites; E2, enzyme form with low affinity for Ca^{2+}; E2(TG), E2 enzyme with bound thapsigargin; E1P, ADP-sensitive phosphoenzyme intermediate containing Ca^{2+} in the occluded state; E2P, ADP-insensitive phosphoenzyme intermediate with luminally facing low affinity Ca^{2+} binding sites; EPPS, *N*-2-hydroxyethylpiperazine-*N*′-3-propanesulfonic acid; $K_{0.5}$, ligand concentration giving half-maximum effect; MES, 2-[*N*-morpholino]ethanesulfonic acid; MOPS, 3-[*N*-morpholino]propanesulfonic acid; TMAH, tetramethylammonium hydroxide; TNP-8N_3-ATP, 2′,3′-*O*-(2,4,6-trinitrophenyl)-8-azidoadenosine 5′-triphosphate.

vided a detailed view of the reaction pathway in the case of phosphoserine phosphatase, and show small progressive structural adjustment of the active site loops and attendant side chains leading to a tight transition state configuration around the phosphoryl group or analog (*cf.* Ref. 5 and Fig. 1*B*). The equivalent residues in E1(Ca_2) and E2(TG) structures of Ca^{2+}-ATPase are further apart compared with those of phosphoserine phosphatase (Fig. 1, compare *A* and *B*), raising the question whether significant gathering or closing around the γ-phosphoryl group or phosphate is required in the ion pump to reach the transition state for phosphoryl transfer. Hence, an important challenge is to reveal such structural changes in the Ca^{2+}-ATPase. Mg^{2+}, which, according to structures of phosphoserine phosphatase and other proteins in this family, is critically situated between the ^{351}DKTGT phosphorylation loop, ^{701}TGDVND loop (with Asp^{703} being strongly involved in ligation), and the phosphoryl group (*cf.* Fig. 1*B*), may be a key component of the tightening. ATP may also be required; the crystals of E1(Ca_2) were grown in the presence of high Mg^{2+} and Ca^{2+}, and yet there was no divalent cation at the putative catalytic Mg^{2+} site near Asp^{351}, possibly because of the absence of ATP. Ca^{2+} binding at the membranous transport sites activates phosphoryl transfer to Asp^{351} and may be another important component required for the tightening to reach the transition state.

The present study expands on our previous studies of domain P mutations, which investigated the role of the conserved phosphorylation loop ^{351}DKTGTLT in MgATP binding (6, 7). We now focus on the other conserved segments of the P domain mentioned above. We have introduced new mutations of some of the conserved residues in these segments, including the putative Mg^{2+} binding residue, Asp^{703}, as well as Lys^{684} and Asp^{707}, and we also reexamine previously studied mutants (8–10), using our recently developed techniques for measurement of nucleotide binding and kinetics of phosphorylation, to assess the roles of these residues in nucleotide and Mg^{2+} binding and stabilization of the Ca^{2+}-activated transition state for phosphoryl transfer. Residues in the highly conserved hinge segments, ^{601}DPPR and ^{359}NQ(R/K)MSV, which link the N and P domains, have been studied to probe interdomain movements and the role of the hinge. Because some of the mutants exhibited very slow or negligible phosphorylation, it was possible to measure ATP binding in the presence of both Mg^{2+} and Ca^{2+}, thereby providing insight in the interaction with ATP in the transition state for phosphoryl transfer.

EXPERIMENTAL PROCEDURES

Mutagenesis and Expression—Oligonucleotide-directed mutagenesis of cDNA encoding the rabbit fast twitch muscle Ca^{2+}-ATPase (SERCA1a isoform) was carried out as described previously (9). For expression, the cDNA in pMT2 vector (11) was transfected into COS-1 cells by calcium phosphate precipitation (12). The microsomal fraction containing expressed wild-type or mutant Ca^{2+}-ATPase was recovered by differential centrifugation (13). The concentration of expressed protein was quantified by a specific enzyme-linked immunosorbent assay (9).

Phosphorylation—Transient kinetic experiments at 25 °C were performed using a Bio-Logic quenched flow module QFM-5 (Bio-Logic Science Instruments, Claix, France) as described (14). The reaction was started by the addition of ATP to the Ca^{2+}-bound Ca^{2+}-ATPase. Other phosphorylation and dephosphorylation experiments were carried out by manual mixing techniques (7). Acid quenching was performed with 0.5–2 volumes of 25% (w/v) trichloroacetic acid containing 100 mM H_3PO_4. The acid-precipitated protein was washed by centrifugation and subjected to SDS-polyacrylamide gel electrophoresis in a 7% polyacrylamide gel at pH 6.0 (15), and the radioactivity associated with the separated Ca^{2+}-ATPase band was quantified by imaging, using a Packard Cyclone™ Storage Phosphor System. The background phosphorylation level was determined in parallel experiments with control microsomes isolated from mock-transfected COS-1 cells.

Assays for Nucleotide Binding—The synthesis of [γ-^{32}P]TNP-8N_3-ATP, the photolabeling of COS-1 cell microsomes containing wild-type or mutant Ca^{2+}-ATPase (at room temperature), the inhibition by ATP, and the quantification of labeled bands by radio-imaging following SDS-polyacrylamide gel electrophoresis were carried out as described previously (16). The concentration of [γ-^{32}P]TNP-8N_3-ATP was $3 \times K_{0.5}$ in the inhibition experiments with ATP.

Tight β,γ-Bidentate Cr(III)ATP (CrATP) Binding—The assay consists of preincubating the Ca^{2+}-ATPase with CrATP at 37 °C and then determining the fraction of enzyme not tightly complexed with CrATP by photolabeling with [γ-^{32}P]TNP-8N_3-ATP in excess EDTA following a large dilution, as described previously (6) and also in the legend to the figure. β,γ-Bidentate CrATP was prepared as described by Dunaway-Mariano and Cleland in method B (17).

Calculations and Data Analysis—The phosphorylation data and the [γ-^{32}P]TNP-8N_3-ATP labeling data were analyzed as detailed previously (14, 16). The "true" dissociation constant for ATP and MgATP binding was calculated using the validated equation for competitive inhibition of the [γ-^{32}P]TNP-8N_3-ATP labeling (16).

RESULTS

The mutants examined are listed in Table I. To follow the results, it is helpful to know the disposition of these residues in the phosphorylation site and roughly how ATP and Mg^{2+} may bind. A model based on the crystal structure of Ca^{2+}-ATPase in the E2(TG) conformation (2), the atomic structure of the homologous phosphoserine phosphatase with bound phosphoserine (5), and an NMR structure of ATP bound to domain N of Na^+,K^+-ATPase (18) is presented in Fig. 1*A*. ATP is shown in *yellow*. The AMP portion of ATP is lodged in domain N, and the β- and γ-phosphates in domain P in a position close to Asp^{351}, the residue receiving the γ-phosphate from ATP. The ATP molecule is stretched between the α- and β-phosphates (indicated by *dashed line*) to reach both sites, and it is apparent that further movement of the two domains is needed for the ATP to straddle both binding sites. This problem is even more pronounced in the E1(Ca_2) Ca^{2+}-ATPase crystal structure (1), which led us to prefer the E2(TG) structure rather than E1(Ca_2) for modeling the ATP binding site. In a transition state-like structure of phosphoserine phosphatase, where AlF_3 is bound as a phosphoryl transition state analog, Mg^{2+} is coordinated by a fluoride atom, the residues equivalent to Asp^{351} and Asp^{703}, the main chain carbonyl of the equivalent of Thr^{353}, and two water molecules (Fig. 1*B*). AlF_3 is ligated to main chain amides of residues equivalent to Lys^{352}, Thr^{353}, and Gly^{626}, as well as to side chains of the equivalents of Thr^{625} and Lys^{684} (Ref. 5 and Fig. 1*B*). Hence, these residues are candidates as ligands of Mg^{2+} and γ-phosphate, respectively, in the transition state of the Ca^{2+}-ATPase.

Nucleotide Binding with and without Mg^{2+} in the Absence of Ca^{2+}—Direct measurement of ATP binding to mutant Ca^{2+}-ATPase expressed in COS-1 cell microsomes is not possible by conventional methods because of the low amount of expressed protein. However, we have developed a binding assay based on specific [γ-^{32}P]TNP-8N_3-ATP photolabeling of Lys^{492} in domain N and its inhibition by ATP, competing for binding (16). Briefly, the concentration dependence of TNP-8N_3-ATP photolabeling provides a $K_{0.5}$ value, which is the concentration at which there is half-maximal photolabeling, and then the ATP concentration dependence of inhibition of photolabeling is studied at a concentration of TNP-8N_3-ATP approximately equal to $3 \times K_{0.5}$. This provides a $K_{0.5}$ value for ATP binding from which the "true" K_D for ATP binding is calculated using the equation for competitive binding. TNP-8N_3-ATP is a substrate for the Ca^{2+}-ATPase both when bound noncovalently and when covalently attached to Lys^{492}, although the hydrolysis is slow for this substrate (19).

The binding parameters obtained with wild type and the mutants are presented in Table I, and examples of the underlying experimental data are shown in Fig. 2. In the table, values of

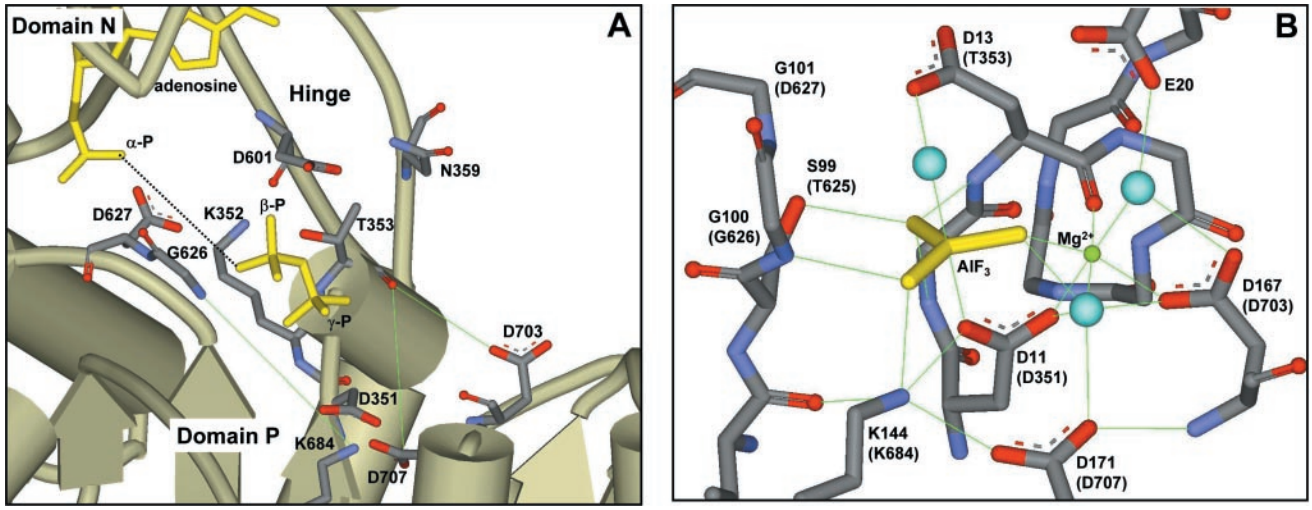

FIG. 1. **Disposition of domain P residues in Ca^{2+}-ATPase (*A*) and of equivalent residues in a pseudotransition state of phosphoserine phosphatase (*B*).** In *A*, the structure of Ca^{2+}-ATPase is that of the E2(TG) crystal structure of Ca^{2+}-ATPase (Ref. 2, PDB accession no. 1IWO). Domain A has been omitted for clarity. A model of an ATP molecule, separated between the α- and β-phosphates (indicated by *dashed line*), is shown in *yellow*. The ATP was taken from an NMR structure of recombinant N domain of Na^+,K^+-ATPase complexed with ATP (Ref. 18, PDB accession no. 1MO8). The AMP portion has been inserted in the Ca^{2+}-ATPase in a position that approximates that of the NMR structure, and the pyrophosphate portion is positioned such that the γ-phosphate approximates the phosphoryl group of phosphoserine in a crystal structure of the homologous phosphoserine phosphatase with bound substrate (Ref. 5, PDB accession no. 1L7P). The *green lines* in *A* indicate distances that need to shorten by 4–5 Å to approach the structure of phosphoserine phosphatase complexed to AlF_3 and Mg^{2+}, which is presented in *B* (Ref. 5, PDB accession no. 1L7N). This structure is thought to mimic the transition state in the phosphoryl transfer reaction (5). The AlF_3 (homolog of the phosphoryl) is shown in *yellow* and Mg^{2+} as a *green ball*. Three of the water molecules present in the crystal are highlighted as *light blue balls*. The *green lines* in *B* show distances of less than 3.2 Å. The equivalent residues of Ca^{2+}-ATPase are indicated in *parentheses*. Both pictures were prepared by use of DS Viewer Pro (Discovery Studio, Accelrys Inc.).

TABLE I
Nucleotide binding and phosphorylation parameters

Photolabeling and inhibition with ATP/MgATP were carried out as described in the legend to Fig. 2 (*cf.* also Ref. 7). Values of $K_{0.5(TNP\text{-}8N3\text{-}ATP)}$ and of $K_{D(ATP)}$ more than 2-fold different from wild type are shown in bold, and, of these, those indicating an increase in affinity are in italics. In the presence of Mg^{2+} + Ca^{2+}, there are no wild-type data to compare with, and comparison is made with parameters of the same mutant in Mg^{2+} alone.

Mutation	Binding in EDTA[a]		Binding in Mg^{2+}/EGTA[b]		Binding in Mg^{2+}/Ca^{2+} [c]		Phosphorylation rate[d] (k_{obs})	Rate of E1P→E2P transition[e] (k_{obs})	Rate of CrATP binding[f]
	$K_{0.5(TNP\text{-}8N3\text{-}ATP)}$	$K_{D(ATP)}$	$K_{0.5(TNP\text{-}8N3\text{-}ATP)}$	$K_{D(ATP)}$	$K_{0.5(TNP\text{-}8N3\text{-}ATP)}$	$K_{D(ATP)}$			
	μM		μM		μM		s^{-1}		
Wild type	0.19	21	0.79	0.51			35	0.23	+++
P domain									
Gly^{626} → Ala	0.28	**47**	**1.6**	**14**	1.4	**>1000**	0.05		−
Asp^{627} → Glu	0.21	19	**2.4**	0.35			16	0.050	
Asp^{627} → Asn	***0.032***	***4***	0.77	**3.8**			6	0.027	−
Lys^{684} → Arg	0.19	27	0.54	**2.4**			1.2	<0.1[h]	
Lys^{684} → Met	***0.039***	***8.3***	***0.036***	**11**	**0.33**	***0.76***	−[g]		−
Asp^{703} → Glu	0.15	29	0.83	0.99			26	0.10	
Asp^{703} → Asn	***0.058***	***7.8***	0.82	**2.5**			16	0.084	+
Asp^{703} → Ala	***0.067***	18	0.47	**3.1**	0.34	**37**	0.07	0.004	+
Asp^{703} → Ser	***0.061***	***8.7***	1.2	**4.2**	***0.40***	7.0	0.11		++
Asp^{703} → Cys	***0.040***	***5.7***	0.86	**2.8**	***0.29***		0.02		+
Asp^{707} → Asn	***0.006***	***1.5***	***0.19***	**1.6**	0.10	***0.34***	−		−
Asp^{707} → Ser	***0.022***	***6.8***	***0.28***	**2.2**	***0.062***	***0.75***	−		+
Asp^{707} → Cys	***0.063***	13	0.41	0.23	***0.2***	**1.6**	−		+
Hinge									
Asn^{359} → Ala	0.21	32	***0.19***	***0.056***			34	0.074	+++
Asp^{601} → Glu	0.23	36	**3.3**	**4.0**			8	0.038	++
Asp^{601} → Asn	***0.068***	13	***0.13***	***0.030***			11	0.063	++

[a] Medium consisted of 25 mM EPPS/TMAH (pH 8.5), 20% (v/v) glycerol, 2 mM EDTA.
[b] Medium consisted of 25 mM EPPS/TMAH (pH 8.5), 20% (v/v) glycerol, 1 mM $MgCl_2$, 0.5 mM EGTA.
[c] Medium consisted of 25 mM EPPS/TMAH (pH 8.5), 20% glycerol, 1 mM $MgCl_2$, 0.05 mM $CaCl_2$.
[d] Data were obtained as described for Fig. 3 (*A* and *B*). The value for Lys^{684} → Arg was reproduced from Ref. 14.
[e] Dephosphorylation rate at 0 °C was determined by chase with nonradioactive ATP and EGTA as described for Fig. 3*C*.
[f] Subjective assessment was made on basis of the data shown in Fig. 4.
[g] Minus sign indicates that the data are indistinguishable from background.
[h] Value is based on the data in Ref. 9.

$K_{0.5(TNP\text{-}8N_3\text{-}ATP)}$ and $K_{D(ATP)}$ more than 2-fold different from wild type are shown in bold type, and, of these, those showing an increase in affinity are in italics. For side chains contributing to ligation of the nucleotide, a reduced affinity is expected upon mutation. For charged side chains, removal of the charge by mutation may lead to an increase of the affinity for the nucleotide, if there is electrostatic repulsion in the wild type. Examining domain P mutations in the absence of Mg^{2+} first, it can be seen that most charge-removing mutations increased the affinity for TNP-$8N_3$-ATP and ATP. This was especially pronounced for

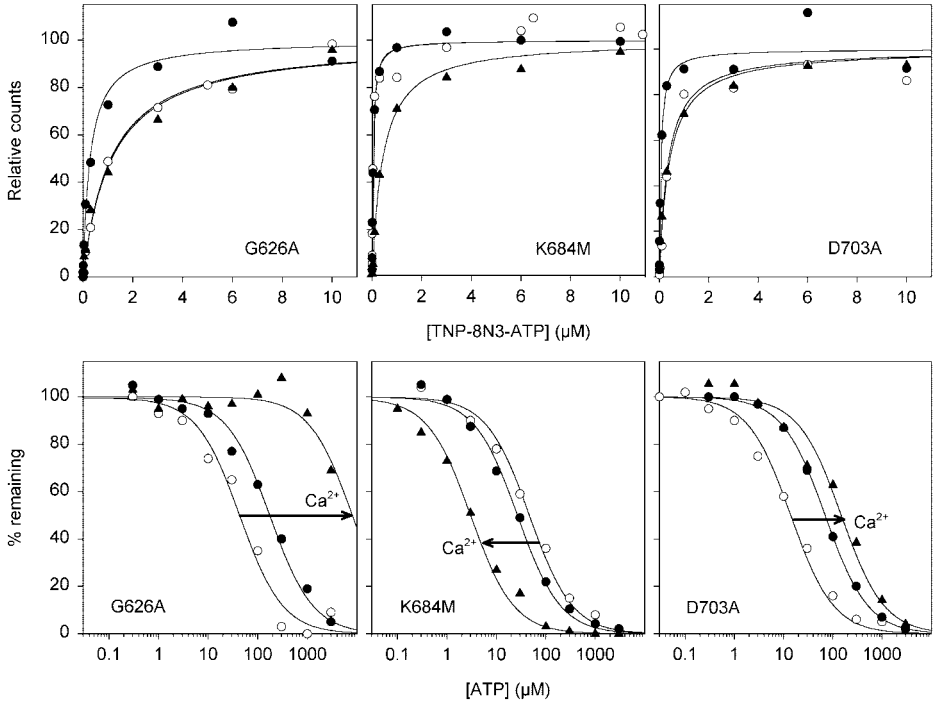

FIG. 2. **TNP-8N_3-ATP photolabeling (*upper panels*) and ATP inhibition (*lower panels*).** Photolabeling was performed with COS-1 cell microsomes in 25 mM EPPS/TMAH, pH 8.5, 20% (w/v) glycerol, variable concentrations of [γ-^{32}P]TNP-8N_3-ATP, and 2 mM EDTA (*closed circles*), 1 mM $MgCl_2$ + 0.5 mM EGTA (*open circles*), or 1 mM $MgCl_2$ + 0.05 mM $CaCl_2$ (*closed triangles*). The samples were subjected to SDS-polyacrylamide gel electrophoresis and the radioactivity associated with the Ca^{2+}-ATPase band quantified. The sum of a hyperbolic function and a linear component was fitted to the data. In the presented data and curves, the linear component has been subtracted. In the ATP inhibition experiments, the concentration of [γ-^{32}P]TNP-8N_3-ATP was close to 3 × $K_{0.5}$ (see Table I), and ATP was included at the concentrations indicated. A simple binding function with an offset representing nonspecific labeling was fitted to the data. The presented data and curves have the offset subtracted. All data sets are the average of two or more experiments. The *arrow* indicates the difference induced by Ca^{2+}.

Asp^{707}→ Asn, where the affinity was increased 33- and 14-fold, respectively. Asp^{707}→ Cys hardly changed the affinity for ATP, which may be taken as an indication that the sulfhydryl group is ionized, thereby maintaining the same electrostatic environment as the aspartate. Rather surprisingly considering their conservation in related enzymes, but in keeping with what has been found for Asp^{351} (6), replacement of Asp^{627} and Asp^{703} with the longer glutamate side chain had no effect on binding of TNP-8N_3-ATP or ATP, suggesting there are no steric clashes. We conclude that in wild type none of the residues appear to be involved in ligation of the phosphates of TNP-8N_3-ATP or ATP in the absence of Mg^{2+}, and mostly electrostatic repulsive forces prevail.

In the presence of Mg^{2+}, a different picture emerges, showing differential mutational effects on TNP-8N_3-MgATP and MgATP binding. Under the conditions applied, ~95% of ATP should exist in the form of the MgATP complex, with a single negative charge. This complex binds to wild-type enzyme with higher affinity than uncomplexed ATP, whereas the Mg^{2+} complex of TNP-8N_3-ATP binds with lower affinity than the uncomplexed nucleotide to the wild type (Table I). Some mutations increased the affinity for TNP-8N_3-MgATP, some had no effect, whereas others mildly decreased the affinity, relative to wild type. The 22-fold increase in TNP-8N_3-MgATP affinity seen for Lys^{684}→ Met is particularly prominent. Increases in TNP-8N_3-MgATP affinity were found for mutations of neighboring Asp^{707}, as well, resembling to some extent the situation in the absence of Mg^{2+}. Mutations of Asp^{703} did not affect TNP-8N_3-MgATP binding. Mg^{2+}, thus, decreased the affinity for TNP-8N_3-ATP even more in the Asp^{703} mutants than in the wild type. Hence, Lys^{684}, Asp^{707}, and Asp^{703} do not contribute to coordination of the Mg^{2+} binding with TNP-8N_3-ATP. In contrast, many domain P mutations decreased the affinity for MgATP. The most critical residues seem to be Gly^{626} and Lys^{684}, for which replacement with alanine and methionine, respectively, led to 28- and 22-fold decrease of MgATP affinity, indicating that the main chain of Gly^{626} and side chain amino group of Lys^{684} play important roles in the ligation of MgATP. In the case of the aspartates, 3–8-fold decreases of affinity were observed for mutations removing the negative charge. It is interesting to note that, in these mutants, there is little difference between the affinities for ATP and MgATP, because the affinity for ATP is increased and the affinity for MgATP decreased, compared with wild type. As seen for ATP, mutation of Asp^{627} or Asp^{703} to glutamate had no significant effect on the affinity for MgATP, again suggesting no steric clashes with the longer side chain. Mutation Asp^{707}→ Cys was also silent, and again this may be because the cysteine is ionized.

Asn^{359} and Asp^{601} are located on the flexible hinge segments linking domains N and P (*cf.* Fig. 1*A*). Mutation of these two residues had little or no effect on ATP binding in the absence of Mg^{2+}, but in the presence of Mg^{2+}, Asn^{359}→ Ala and Asp^{601}→ Asn caused pronounced increases in affinity for both nucleotides, whereas Asp^{601}→ Glu was detrimental.

Phosphorylation from [γ-^{32}P]ATP and Phosphoenzyme Turnover—In the presence of Ca^{2+}, the interaction with MgATP normally leads to phosphoryl transfer to Asp^{351} with resulting formation of the ADP-sensitive phosphoenzyme intermediate, E1P. It was previously reported that Asp^{601}→ Glu, Gly^{626}→ Ala, Asp^{703}→ Ala, and Asp^{707}→ Asn are unable to form significant amounts of phosphoenzyme upon incubation with 2 μM [γ-^{32}P]ATP and Ca^{2+} for 10 s at 0 °C, whereas Asp^{601}→ Asn, Asp^{627}→ Glu, Lys^{684}→ Arg, Asp^{703}→ Glu, and Asp^{703}→ Asn form a phosphoenzyme under these conditions (8–10). We were able to confirm these findings, except for Asp^{601}→ Glu, which phosphorylated to a wild type-like level in our hands. With respect to those mutants that have not been previously studied, we observed wild type-like accumulation of phosphoenzyme in the case of Asn^{359}→ Ala and Asp^{627}→ Asn, whereas Lys^{684}→ Met, Asp^{703}→ Cys, Asp^{703}→ Ser, Asp^{707}→ Cys, and Asp^{707}→ Ser were unable to form a significant amount of phosphoenzyme when incubated with 2 μM [γ-^{32}P]ATP and Ca^{2+} at 0 °C. We then proceeded to study the rate of phosphorylation at 25 °C, using a quenched flow procedure (14). At 25 °C, all the mutants, except Lys^{684}→ Met and the three mutants with alteration to Asp^{707}, were capable of undergoing measurable phosphorylation from [γ-^{32}P]ATP in the presence of Mg^{2+} and Ca^{2+} (E1 → E1P transition). Examples of data obtained under these conditions are shown in Fig. 3 (*A* and *B*), and all the observed rate constants are listed in Table I. It should be understood that, because the MgATP concentration applied (5

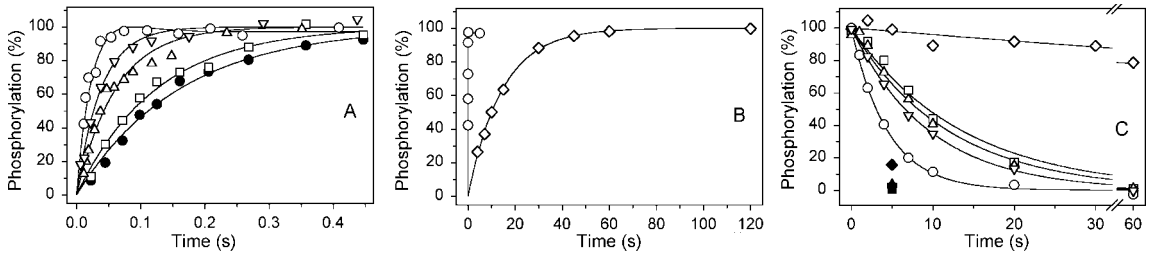

FIG. 3. **Phosphoenzyme formed from [γ-^{32}P]ATP.** *A*, phosphorylation of mutants Asp^{601}→ Glu (*squares*), Asp^{627}→ Asn (*solid circles*), Asp^{703}→ Asn (*triangles pointing upward*), Asp^{703}→ Glu (*triangles pointing downward*) and wild type (*open circles*) was carried out at 25 °C in a medium containing 40 mM MOPS/Tris (pH 7.0), 80 mM KCl, 100 μM $CaCl_2$, 5 mM $MgCl_2$, and 5 μM [γ-^{32}P]ATP. The samples were acid quenched at serial time intervals, using a Bio-Logic QFM-5 quench-flow module with mixing protocol as previously described (14), and further processed as described under "Experimental Procedures." The data for the wild type and each mutant were normalized separately, taking the maximum level of phosphorylation as 100%. For the mutants, the *lines* show the best fits of a monoexponential function to the data, the rate constants being listed in Table I. *B*, phosphorylation and data analysis were carried out as described above, except that a manual mixing technique was used for mutant Asp^{703}→ Ala (*diamonds*); note the time scale. The *circles* reproduce the wild-type data from *panel A* for direct comparison. *C*, E1P → E2P transition. Phosphorylation was carried out for 15 s at 0 °C (wild type, Asn^{359}→ Ala, Asp^{703}→ Asn, and Asp^{703}→ Glu) or for 30 s at 25 °C followed by cooling on ice for 30 s (Asp^{703}→ Ala, because of its inability to phosphorylate at 0 °C) in 40 mM MOPS/Tris (pH 7.0), 80 mM KCl, 5 mM $MgCl_2$, 1 mM EGTA, 0.955 mM $CaCl_2$ (resulting in 10 μM free Ca^{2+}), 2 μM calcium ionophore A23187, and 5 μM [γ-^{32}P]ATP. To follow dephosphorylation, the phosphoenzyme was chased at 0 °C by addition of 6.7 mM EGTA with either 1 mM nonradioactive ATP (*open symbols*) or 1 mM ADP (*closed symbols*), and acid quenching was performed at the indicated time intervals. The *lines* show the best fits of a monoexponential decay function, giving the rate constants listed in Table I. *Symbols* are as for *panels A* and *B*, except that *squares* represent Asn^{359}→ Ala.

μM) is close to the K_m for phosphorylation of wild type, changes in the affinity for MgATP as well as the V_{max} for phosphorylation are being reflected in the phosphorylation rate.

In the hinge segments, mutation Asn^{359}→ Ala had no effect on the phosphorylation rate, whereas both mutations of Asp^{601} slowed phosphorylation. A moderate slowing of the phosphorylation rate at 25 °C was also recorded for mutations of Asp^{627}. Mutation Gly^{626}→ Ala and mutation of Asp^{703} to alanine, cysteine, or serine reduced the rate of phosphorylation several hundredfold (*cf.* Table I and Fig. 3*B*, showing the data for Asp^{703}→ Ala), whereas the more conservative changes of Asp^{703} to asparagine and glutamate only reduced the phosphorylation rate to 46 and 74%, respectively, compared with wild type (Fig. 3*A* and Table I).

It is remarkable that phosphoenzyme did accumulate in Asp^{703}→ Ala/Cys/Ser, despite the low rate of phosphorylation, suggesting that a step in the reaction sequence leading to dephosphorylation is also blocked. This was further examined for Asp^{703}→ Ala, and, as seen in Fig. 3*C*, the dephosphorylation observed upon chase of the phosphoenzyme with nonradioactive ATP was unusually slow. A rapid dephosphorylation was, on the other hand, observed upon addition of ADP to reverse the phosphorylation step, indicating that the accumulated phosphoenzyme intermediate was ADP-sensitive E1P and that the slow step in the forward dephosphorylation is the E1P → E2P conformational transition.

Among the mutants studied, only Asn^{359}→ Ala and Asp^{703}→ Glu showed Ca^{2+} transport activity higher than 10% of wild type in the presence of a high MgATP concentration of 5 mM at 37 °C (50 and 30%, respectively; data not shown; assay carried out as described in Ref. 20). A block or slowing of the E1P → E2P transition has previously been described for mutants Asp^{601}→ Asn, Lys^{684}→ Arg, Asp^{703}→ Asn, and Asp^{627}→ Glu, on the basis of measurements similar to those shown in Fig. 3*C* (8, 9). We confirmed these results and, furthermore, observed a marked inhibition of the E1P → E2P transition in Asp^{601}→ Glu and Asp^{627}→ Asn, and a less pronounced slowing in Asn^{359}→ Ala and Asp^{703}→ Glu (Fig. 3*C* and Table I). Because E1P → E2P normally is the rate-limiting step in the transport cycle at saturating ATP and Ca^{2+} concentrations, the inhibition of this step must contribute, besides a reduced phosphorylation rate, to reduce the Ca^{2+} transport activity in the mutants.

Nucleotide Affinity in the Presence of Ca^{2+}—In the presence of both Mg^{2+} and Ca^{2+}, TNP-8N_3-ATP is a substrate of the Ca^{2+}-ATPase (19). Hence, it is normally not possible to measure TNP-8N_3-ATP or ATP binding by the photolabeling assay under these conditions, because the γ-phosphoryl group would be cleaved off, both from TNP-8N_3-ATP and from the ATP used to competitively inhibit the photolabeling. However, for the mutants exhibiting no or very low phosphorylation activity, the assay could be employed with both Mg^{2+} and Ca^{2+} present, *i.e.* the conditions where the transition state in the phosphoryl transfer reaction normally would be attained. Results are shown in Fig. 2 and Table I. With respect to TNP-8N_3-ATP binding, a pronounced Ca^{2+} effect was noticed only for Lys^{684}→ Met, where the binding affinity was lowered ~10-fold relative to the situation without Ca^{2+}. There were slight increases in affinity for the Asp^{703} and Asp^{707} mutants, the 4-fold increase in affinity seen for Asp^{707}→ Ser clearly being significant. In the case of ATP, the Ca^{2+}-induced changes were quite dramatic and surprising for some of the mutants. In Fig. 2, the *arrow* indicates the effect of Ca^{2+}. In Gly^{626}→ Ala, the ATP affinity was very low in the presence of Ca^{2+}, ~100-fold reduced relative to the situation with Mg^{2+} alone. Ca^{2+} lowered the ATP affinity 12-fold in Asp^{703}→ Ala. In contrast, Ca^{2+} increased the ATP affinity 14-fold in Lys^{684}→ Met. Similarly, 3- and 5-fold increases in ATP affinity were observed for Asp^{707}→ Ser and Asp^{707}→ Asn, respectively (Table I). Mutant Asp^{707}→ Cys was again the exception, Ca^{2+} lowering the affinity 7-fold. Ca^{2+} had little effect on Asp^{703}→ Ser. In Asp^{703}→ Cys, Ca^{2+} produced a biphasic inhibition curve, which is difficult to interpret (data not shown). It should be noted that in these experiments the Mg^{2+} concentration was 20-fold higher than the Ca^{2+} concentration, thus ensuring that the major part of the nucleotide was still present as the Mg^{2+} complex. Hence, the changes induced by Ca^{2+} are caused by Ca^{2+} binding at the transport sites.

Tight Binding of CrATP—The roles of these residues in nucleotide binding were further investigated by determining the rate at which CrATP becomes tightly bound at the active site in the presence of Ca^{2+} (21, 22). We have previously demonstrated that it is possible to determine the time course of tight CrATP binding in an assay in which the enzyme is preincubated with CrATP at 37 °C for various times followed by dilution into medium containing TNP-8N_3-ATP, which photolabels the enzyme fraction not having CrATP tightly bound (6). Results obtained using this assay are shown in Fig. 4 and summarized in Table I. Each of the panels shows photolabeling following preincubation for various times in the absence (*open circles*) and presence (*closed circles*) of CrATP. In the presence of CrATP, the disappearance of the ability to become photola-

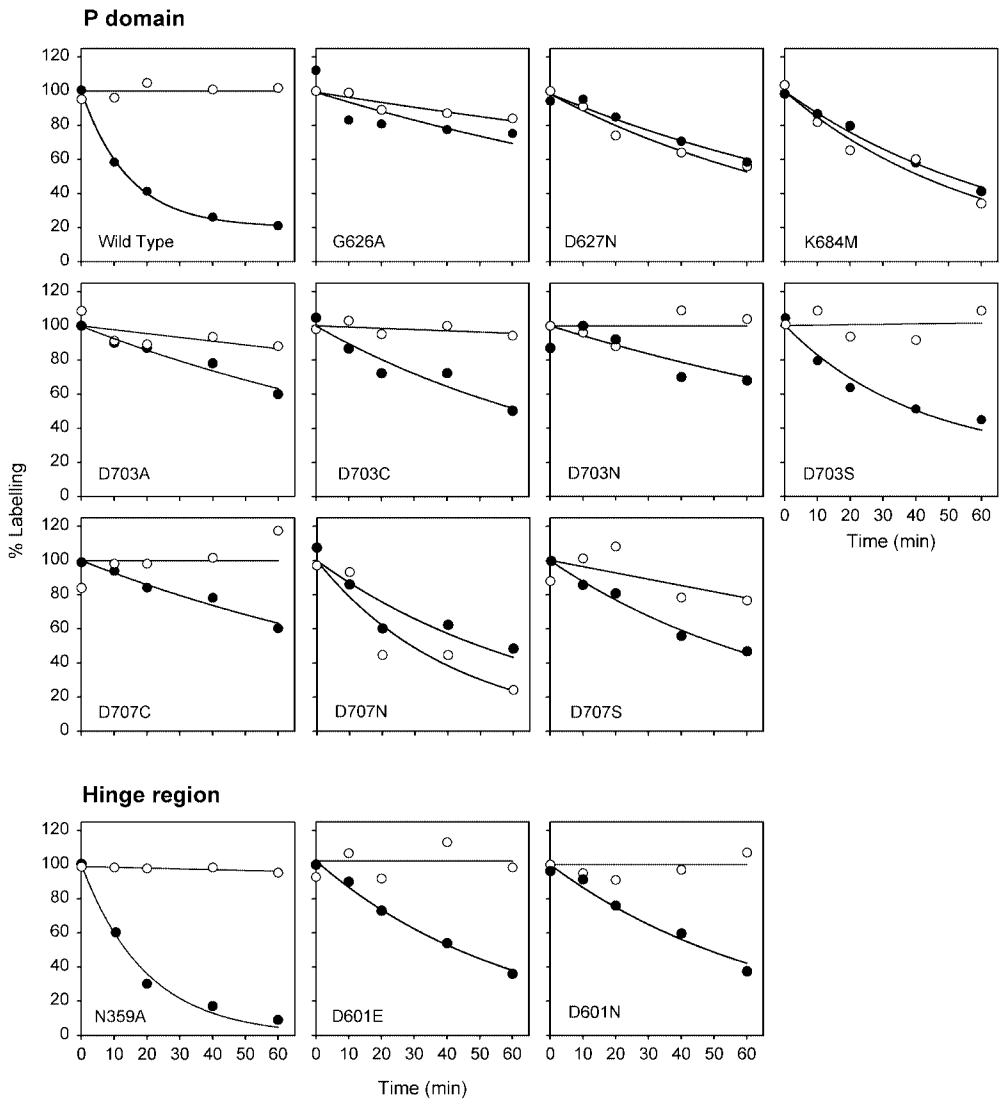

FIG. 4. **Tight CrATP binding.** The microsomes were incubated at 37 °C in 50 mM MOPS/TMAH, pH 7.0, 100 mM NaCl, 2 mM $MgCl_2$, 0.2 mM $CaCl_2$, with (*solid circles*, test) or without (*open circles,* control) 0.84 mM CrATP. At the indicated times, aliquots were diluted 15.6-fold into ice-cold irradiation medium containing 25 mM EPPS/TMAH, pH 8.5, 2 mM EDTA, 20% (w/v) glycerol, [γ-^{32}P]TNP-8N_3-ATP at a concentration of $3 \times K_{0.5}$, and either no CrATP (test) or 0.054 μM CrATP (control) and irradiated immediately. The samples were then subjected to SDS-polyacrylamide gel electrophoresis, and the radioactivity associated with the Ca^{2+}-ATPase band quantified.

beled (*i.e.* the formation of the complex with CrATP) took place with a $t_{1/2}$ of ~10 min for wild-type enzyme, whereas in the absence of CrATP the photolabeling level remained steady over the time course. For $Gly^{626} \rightarrow$ Ala, there was little effect of CrATP, indicating that no tight complex with CrATP was produced. $Asp^{703} \rightarrow$ Ala/Cys/Asn/Ser and $Asp^{707} \rightarrow$ Cys/Ser showed some effect of CrATP, but clearly the formation of the tight complex was slower in these mutants compared with wild type. In the hinge, the two mutations of Asp^{601} moderately slowed the formation of the tight complex, and $Asn^{359} \rightarrow$ Ala was like wild type. For $Asp^{627} \rightarrow$ Asn, $Lys^{684} \rightarrow$ Met, and $Asp^{707} \rightarrow$ Asn, a fall off in labeling with time was noted even in the absence of CrATP. The presence of CrATP did not enhance this decline; therefore, none of these mutants appeared to produce a tight complex with CrATP.

Mg^{2+} and P_i Concentration Dependence of Phosphorylation from P_i in $Asp^{703} \rightarrow Glu$—In the presence of Mg^{2+}, but without Ca^{2+}, the Ca^{2+}-ATPase in E2 conformation can be phosphorylated by inorganic phosphate in a reaction reversing the dephosphorylation of E2P occurring in the transport cycle. Among the mutants examined in the present study, only $Asn^{359} \rightarrow$ Ala, $Asp^{601} \rightarrow$ Glu, $Asp^{601} \rightarrow$ Asn, $Asp^{627} \rightarrow$ Glu, and $Asp^{703} \rightarrow$ Glu were phosphorylated by $^{32}P_i$ under conditions that are optimal in wild type (incubation with $^{32}P_i$ and Mg^{2+} for 10 min at 25 °C, pH 6.0, in the presence of 30% dimethyl sulfoxide). Data obtained with $Asp^{703} \rightarrow$ Asn and $Asp^{703} \rightarrow$ Glu are shown in Fig. 5. For $Asp^{703} \rightarrow$ Glu, the apparent affinities for P_i and Mg^{2+} could be determined and compared with wild type. It is seen in Fig. 5 that the apparent affinity for P_i is approximately 4-fold reduced relative to wild type, whereas the apparent affinity for Mg^{2+} is reduced as much as 14-fold. We conclude that even the addition of a methylene group to the side chain of Asp^{703} causes a marked perturbation of the interaction with Mg^{2+} in the E2 conformation. For $Asp^{703} \rightarrow$ Asn, an increase of the Mg^{2+} concentration to as much as 50 mM did not allow accumulation of a significant amount of phosphoenzyme.

DISCUSSION

In the present study we have demonstrated that Mg^{2+} and Ca^{2+} (binding at the catalytic site and transport sites, respectively) have conspicuous effects on the interaction of the Ca^{2+}-ATPase with nucleotide, and our results pinpoint residues involved in these effects.

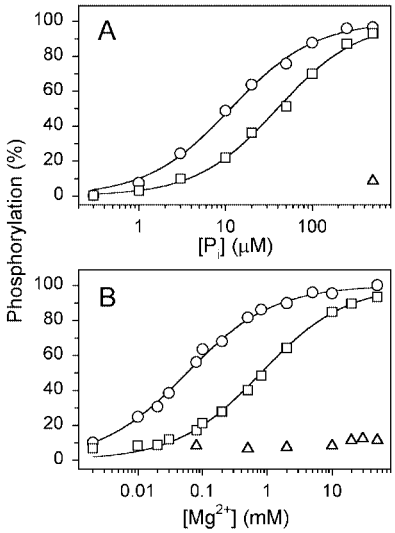

FIG. 5. **Effect of Asp^{703} mutations on P_i and Mg^{2+} concentration dependence values of phosphorylation from $^{32}P_i$.** The reaction was performed for 10 min at 25 °C in 100 mM MES/Tris (pH 6.0), 2 mM EGTA, 30% (v/v) dimethyl sulfoxide, and either (*A*) 10 mM $MgCl_2$ and varying concentrations of $^{32}P_i$ or (*B*) 0.5 mM $^{32}P_i$ and varying concentrations of $MgCl_2$. The *lines* show the best fits of the equation, $EP = EP_{max}\cdot[P_i]^n/(K_{0.5} + [P_i]^n)$ to the data, giving the $K_{0.5}$ values indicated in parentheses: *circles*, wild type ($K_{0.5}(P_i)$ 11 μM, $K_{0.5}(Mg^{2+})$ 58 μM); *squares*, $Asp^{703}\rightarrow$ Glu ($K_{0.5}(P_i)$ 40 μM, $K_{0.5}(Mg^{2+})$ 805 μM); *triangles*, $Asp^{703}\rightarrow$ Asn (no significant phosphorylation).

Electrostatic Effects and Role of Mg^{2+} in Nucleotide Binding—A large difference was found between mutational effects on nucleotide binding in the absence and presence of Mg^{2+}. In the absence of Mg^{2+}, mutations removing the charges of domain P residues Asp^{627}, Lys^{684}, Asp^{703}, and Asp^{707} mostly enhanced TNP-8N_3-ATP and ATP binding, suggesting proximity of the phosphate chain to these residues in the wild type, but not ligation. In the presence of Mg^{2+}, these mutations, as well as $Gly^{626}\rightarrow$ Ala, were inhibitory for ATP binding, suggesting that in the wild type there is close favorable interaction of these residues with MgATP, *i.e.* ligation. For TNP-8N_3-ATP, only mutations of the ^{625}TGD loop were inhibitory in the presence of Mg^{2+}, placing the phosphate chain of the photolabel at some distance from the other P domain residues under these conditions. Mutations of the hinge residues, Asn^{359} and Asp^{601}, had quite large effects on ATP binding in the presence of Mg^{2+}, and only smaller effects on binding in the absence of Mg^{2+}.

On the basis of the atomic structure of phosphoserine phosphatase in a transition state-like configuration (Ref. 5 and Fig. 1*B*), domain P of Ca^{2+}-ATPase must undergo substantial rearrangements from the known E1(Ca_2) and E2(TG) atomic structures for phosphorylation to occur. Hence, the distances between the backbone carbonyl of Thr^{353} and the carboxyls of Asp^{703} and Asp^{707}, and that between the amide of Gly^{626} and the amino group of Lys^{684} need to shorten by 4–5 Å, if they are to approach the transition state configuration of the phosphatase (see *green lines* in Fig. 1*A*). A further necessary adjustment involves Asp^{351}. The carboxyl is turned "downward," away from the expected approach of the γ-phosphoryl group of ATP, and needs to rotate upward for an in line attack and also for ligation of Mg^{2+}, as in the transition state of the phosphatase (Fig. 1, compare *A* and *B*). Part of the difficulty in gathering these residues closer is the strong negative electrostatic potential; three aspartates, Asp^{351}, Asp^{703}, and Asp^{707}, surround one lysine, Lys^{684}. On the other side of the phosphorylation well are Lys^{352}, Asp^{601}, and Asp^{627}. The phosphate chain of ATP, if placed in the vicinity, would obviously exacerbate the electrostatic imbalance. Mutagenesis of these conserved domain P residues should be interpreted against the background of strong electrostatic effects within a network of interactions. Eliminating the charge on one residue is bound to influence neighbors and possibly beyond. Lys^{684} is positioned midway between Asp^{351} and Asp^{707} in the crystal structures, and eliminating the charge on the lysine can be expected to change the pK_a of the carboxyls so that one (or both) could become protonated and lose the charge. Eliminating the charge on one of the aspartates may do the same to the lysine. In line with this, there are similarities between the effects of replacement of either Lys^{684} or Asp^{707}.

The present data together with those obtained previously for mutations of the phosphorylation loop, ^{351}DKTGTLT (6, 7), suggest that the main gathering movements of conserved domain P residues is a cooperative effect of ATP and Mg^{2+} binding, and that Ca^{2+} binding at the transport sites provides further structural adjustments to reach the tight ligation needed in the transition state. Without ATP, Mg^{2+} and Ca^{2+} do not achieve the structural changes alluded to above in domain P, as the crystal structures show (1, 2). ATP alone seems to mainly experience electrostatic repulsion, as expected with the existence of a strong negative electrostatic potential at the phosphorylation site. The electrostatic effects on ATP binding in the absence of Mg^{2+} and Ca^{2+} are quite large, with more than 10-fold increases in affinity for mutations $Asp^{351}\rightarrow$ Asn (6) and $Asp^{707}\rightarrow$ Asn (Table I). The effect with the latter mutation was even larger for the TNP nucleotide (33-fold change). Even mutation $Lys^{684}\rightarrow$ Met increased the affinity for both ATP and TNP nucleotide, and this may be the result of linked partial protonation of neighboring Asp^{351} and Asp^{707} as mentioned above. Electrostatic effects seem to extend to Asp^{627}, a bit out of the phosphorylation well itself, where a 5-fold increase of affinity was found upon elimination of the charge. Thus, in the absence of Mg^{2+}, the phosphate chain of both TNP-8N_3-ATP and ATP seems to come into proximity of these aspartates, but repulsive effects prevent ligation. The phosphates likely interact at Lys^{492} and Arg^{489} in domain N, according to our previous mutational analysis (20), and at neighboring Arg^{678} stretching from domain P (23).

Mg^{2+} creates favorable interactions for ATP binding in domain P, because the mutations here were consistently detrimental in the presence of Mg^{2+} and absence of Ca^{2+}, apart from $Asp^{707}\rightarrow$ Cys (the cysteine may be ionized) and charge conserving mutations of the other two aspartates to glutamate. Replacement of Lys^{684} with methionine was severely detrimental for MgATP binding in the absence of Ca^{2+} (22-fold reduction of the affinity, Table I), compatible with Lys^{684} bonding the γ-phosphoryl group in the wild-type Ca^{2+}-ATPase as in phosphoserine phosphatase (*cf.* Fig. 1*B*). Of particular interest is also the inhibition of MgATP binding caused by most mutations of Asp^{703}, which is considered a putative Mg^{2+} coordinating residue on the basis of the phosphoserine phosphatase model (Ref. 5 and Fig. 1*B*). In the absence of Ca^{2+}, MgATP affinity was reduced 5–8-fold by replacement of Asp^{703} with alanine, cysteine, asparagine, or serine, whereas ATP affinity was not reduced. Because the replacement with asparagine produced a change in MgATP affinity similar to that seen with alanine, it appears that the negatively charged carboxylate group of the Asp^{703} side chain is required for proper MgATP ligation in the absence of Ca^{2+}. Replacement of Asp^{703} with glutamate resulted in little inhibition of MgATP binding, indicating little or no steric constraint around this residue in the E1 form, which is compatible with the relative isolation of this side chain in the atomic structures and its exposure to the aqueous medium in the homologous phosphoserine phosphatase structures. The phosphorylation of the E2 form with inorganic phosphate was very sensitive to mutations of Asp^{703} (Fig. 5), and even

the replacement with glutamate induced a large (14-fold) reduction of the apparent affinity for Mg^{2+} as activator of phosphorylation by P_i, consistent with a critical role of Asp^{703} in Mg^{2+} ligation in the E2P phosphoenzyme intermediate. For Asp^{707}→ Asn/Ser and Asp^{627}→ Asn, 3–8-fold reductions of MgATP affinity, relative to wild type, were observed in the absence of Ca^{2+}. In these mutants, as well as most of the Asp^{703} mutants, the increased affinity for ATP and the reduced affinity for MgATP translate into little or no difference between the affinities for ATP and MgATP. Hence, the binding data do not permit distinction between the roles of Asp^{703}, Asp^{707}, and Asp^{627} in MgATP binding. In all three cases, perturbation of favorable interaction may be masked by the simultaneous reduction of repulsive forces resulting from the elimination of the negative charge. In phosphoserine phosphatase, Asp^{627} is replaced by glycine (*cf.* Fig. 1*B*). A role for the aspartate in P-type ATPases might be to help fix domains N and P together, and at the same time this residue could interact with the β-phosphate of bound ATP (*cf.* Fig. 1*A*). In phosphoserine phosphatase, the aspartate corresponding to Asp^{707} is within hydrogen bonding distance to a water molecule coordinating Mg^{2+} and, moreover, appears to stabilize the backbone in a conformation allowing the equivalent of Asp^{703} to coordinate Mg^{2+} (*cf.* Fig. 1*B*). A similar scenario in Ca^{2+}-ATPase would be consistent with the present finding of rather similar reductions in MgATP binding affinity for Asp^{707} and Asp^{703} mutations removing the negative charge.

In the case of TNP-$8N_3$-MgATP, mutations Asp^{707}→ Asn/Ser enhanced binding, which not only shows that electrostatic repulsive effects need to be considered, but also demonstrates that Asp^{707} does not contribute to coordination of the Mg^{2+} ion of TNP-$8N_3$-MgATP. Mutation Lys^{684}→ Met also enhanced TNP-$8N_3$-MgATP binding, in line with the hypothesis that the γ-phosphoryl of this nucleotide does not reach this far into the well. Not even mutation of Asp^{703} perturbed the binding of TNP-$8N_3$-MgATP. It appears that, in contrast to the situation with ATP, Mg^{2+} does not anchor the phosphate chain of TNP-$8N_3$-ATP, thus confirming the notion that these two nucleotides are bound differently, although at overlapping sites (20).

CrATP, on the other hand, appears to bind much like MgATP, because the P domain mutations found to inhibit MgATP binding also eliminated or slowed formation of the tight enzyme complex with CrATP. Presumably, the chromium(III) ion takes a position similar to that of the Mg^{2+} of MgATP, with the phosphates reaching into the phosphorylation well. This would also be consistent with our previous finding that mutation of Asp^{351} eliminates tight CrATP binding (6). It should, however, be emphasized that the γ-phosphoryl group of CrATP is not transferred to Asp^{351} in the wild-type enzyme, even though the enzyme-CrATP complex, just as the E1P phosphoenzyme, has Ca^{2+} bound in an occluded state at the transport sites (21, 22), thus indicating that with chromium(III) replacing Mg^{2+} the transition state for phosphoryl transfer cannot be fully reached. The tight binding of CrATP likely results from exchange of one or more of the intramolecular ligands associated with the chromium(III) ion (four water molecules and the β- and γ-phosphates) with oxygen or nitrogen functionalities of the protein, derived from Asp^{351} (6) and, probably, from some of the P domain residues studied here.

The Ca^{2+}-activated Transition State—The negligible phosphorylation activity of several of the mutants provided an opportunity to investigate the energetics in the pseudo-transition state reached in the presence of both Mg^{2+} and Ca^{2+}. Ca^{2+} binding produced large and contrasting changes in MgATP affinity for some of the mutants, compatible with a closer approach of the residues around the phosphates and Mg^{2+}.

Previously, we found that mutant Asp^{351}→ Asn, which is also inactive in phosphorylation, exhibits a very high affinity for ATP in the presence of Mg^{2+} (K_D = 6.5 nM), and the addition of Ca^{2+} lowers the affinity (K_D = 28 nM) (6). For Asp^{351}→ Ala, the reverse is true, the affinity is not so high with Mg^{2+} alone (K_D = 25 nM) and increases with both Ca^{2+} and Mg^{2+} present (K_D = 1.1 nM) (6). These changes are instructive for what is happening at the phosphorylation site in the transition state and for interpretation of the present results. Evidently, the amino group of the asparagine is less perturbing compared with alanine in the ground state, but the larger side chain is more damaging in the tight activated state. Thus, rather minor differences in side chain size can have quite large effects on MgATP binding in a compacted transition state. Even though the Asp^{351} side chain receives the phosphoryl group from ATP, this residue does not appear to be required for the structural rearrangement and favorable interaction with MgATP involved in stabilization of the transition state for phosphoryl transfer, because a large increase of nucleotide affinity occurred upon Ca^{2+} binding in the Asp^{351}→ Ala mutant. It seems likely that a similar increase of favorable interaction with MgATP occurs in the transition state in wild-type enzyme, although this cannot be measured because of the activation of phosphoryl transfer in the wild type. By contrast, Ca^{2+} is expected to lower the MgATP binding affinity in mutants with alterations to residues participating in favorable interaction with the nucleotide in the transition state.

In the case of mutation Lys^{684}→ Met, the affinity for MgATP increased 14-fold on the addition of Ca^{2+}, which is rather similar to the change mentioned above for Asp^{351}→ Ala (23-fold). Thus, even though the affinities for MgATP are very different in the Asp^{351} and Lys^{684} mutants, both express a large affinity increase upon Ca^{2+} binding, and neither of these residues, therefore, seems required for the favorable interaction with nucleotide induced by Ca^{2+} in the transition state. With neighboring Asp^{707}, the serine and alanine mutants showed only 3- and 5-fold increases of the affinity for MgATP, respectively, on the addition of Ca^{2+}, indicating partial tightening, but possibly interference with and, thus, involvement of Asp^{707} in transition state stabilization. The involvement of Asp^{707} is also indicated by the 7-fold reduction of MgATP affinity seen for Asp^{707}→ Cys upon Ca^{2+} binding.

A spectacular 12-fold decrease of MgATP affinity was found upon addition of Ca^{2+} in Asp^{703}→ Ala, strongly suggesting that the presence of Asp^{703} is required for the Ca^{2+}-induced increase of MgATP affinity described above. Hence, Asp^{703} appears to play a more critical role in MgATP binding in the transition state for phosphoryl transfer reached in the presence of Ca^{2+} than in the enzyme complex with MgATP formed in the absence of Ca^{2+}. In the wild type, Ca^{2+} binding at the transport sites may facilitate very tight Mg^{2+} coordination by Asp^{703} in the presence of nucleotide, thereby activating the phosphoryl transfer. Interestingly, the replacement of Asp^{703} with asparagine only moderately slowed phosphorylation, in contrast to the almost complete block of phosphorylation seen for Asp^{703}→ Ala/Ser/Cys, indicating that a carboxamide group can partially substitute for carboxylate in the Ca^{2+}-activated state. It thus seems likely that in the transition state the side chain of Asp^{703} only contributes one oxygen atom directly to Mg^{2+} coordination, as in phosphoserine phosphatase (*cf.* Fig. 1*B*).

The consequences of mutation Gly^{626}→ Ala are especially instructive in evaluating the effects of Mg^{2+} and Ca^{2+} on phosphate anchoring. The interpretation of the results of replacement of this residue is not complicated by electrostatic effects, and the mutation hardly affected nucleotide binding in the absence of Mg^{2+}, indicating weak or no interaction with the phosphate chain, again suggesting that the latter is not in the phosphorylation well under these conditions. Addition of Mg^{2+}

caused the mutation to become strongly perturbing (28-fold decrease in affinity for ATP), and even more significant is the finding that Ca^{2+} binding at the transport sites virtually prevented ATP binding to the Gly^{626}→Ala mutant. Thus, in agreement with the model in Fig. 1*A* and the phosphatase transition state structure in Fig. 1*B*, our data are consistent with the phosphate chain interacting with the amide of Gly^{626} in the presence of Mg^{2+} and Ca^{2+}. Evidently, Ca^{2+} binding in the presence of nucleotide induces quite a dramatic change in the binding site in the vicinity of Gly^{626} that is not apparent by comparison of the E1(Ca_2) and E2(TG) crystal structures. In this connection it is interesting to note that activation of CheY, a response regulator with active site configuration similar to Ca^{2+}-ATPase, likewise involves a significant conformational change here with the residue equivalent to Thr^{625} repositioned to ligate the phosphate or analogue (24).

Roles of P Domain Residues in E1P → E2P Transition—It is striking that mutation of any of the charged residues in domain P that were found important for MgATP or CrATP binding also affected the E1P → E2P transition (stabilized E1P). This finding suggests that the unfavorable electrostatic environment in domain P alluded to above plays a role in the dissociation of ADP and destabilization of E1P conformation causing the relaxation to E2P (release of domain N and rebinding in a different orientation). In line with this hypothesis, the acceleration of the E1P → E2P transition induced by secondary binding of ATP with low affinity to the phosphoenzyme ("modulatory effect") may be the result of unfavorable electrostatic interactions associated with packing an extra phosphate group into the phosphorylated catalytic site in E1P after the dissociation of ADP (20). The mutational effects on the E1P → E2P transition could also be related to changes in Mg^{2+} coordination, as Mg^{2+} binding is required for a normal rate of the E1P → E2P transition (25). Again the difference between the Asp^{703}→ Ala and Asp^{703}→ Asn mutants is noteworthy, the latter showing a 20-fold higher rate of E1P → E2P transition than the former, thus indicating that in the E1P phosphoenzyme, as in the transition state for phosphoryl transfer, a carboxamide group can partially substitute for the carboxylate.

The Hinge Residues—Asp^{601} and Asn^{359} are located in the hinge segments and are at the fulcrum of N-P interdomain movements. Mutations here should impact on partial reactions of the catalytic cycle in which such movements are critical and rate-limiting. We found that the binding of either TNP-$8N_3$-ATP or ATP was only affected with Mg^{2+} present, suggesting that Mg^{2+} is required for fastening of domain N over domain P. This result fits very well with Mg^{2+} inducing favorable interactions of the phosphate chain with critical domain P residues. Both mutations Asn^{359} → Ala and Asp^{601} → Asn enhanced MgATP binding, indicating that some impediment to binding exists in the wild type in this hinge region. The strain could be important for release of domain N and ADP dissociation following phosphorylation, which would be consistent with the reduced rate of the E1P → E2P transition in these mutants. Mutation Asp^{601}→ Glu was quite perturbing for both TNP-$8N_3$-ATP and ATP binding in the presence of Mg^{2+}, as well as for the E1P → E2P transition, showing that steric factors become important at the fulcrum of the hinge when the domains fasten together in connection with nucleotide binding and in the ensuing conformational rearrangement. Despite their opposite effects on MgATP affinity, both mutations of Asp^{601} slowed the rate of phosphorylation from ATP, and mutation Asn^{359}→ Ala had no effect on phosphorylation, despite the increased affinity for MgATP in this mutant, thus adding to the evidence that further Ca^{2+}-induced rearrangement of domains N and P beyond that involved in the anchoring of the phosphate chain is required to reach the transition state in the subsequent phosphorylation step.

Concluding Comments—The present results have pinpointed the important roles of catalytic Mg^{2+} and conserved P domain and hinge residues in anchoring the phosphate chain of ATP. Ca^{2+} binding provokes marked changes in the interaction of Gly^{626} and Asp^{703} with MgATP, and structural rearrangements in domain P seem part of the cue for mediating entry into the transition state for phosphoryl transfer from ATP. The changes in domain P appear to be a cooperative effect of ATP, Mg^{2+}, and Ca^{2+} binding. Coupling of binding of the transported ions to gaining the transition state at the active site is fundamental to P-type ATPases as transport proteins and contributes to distinguishing them from the catalytically related, soluble phosphotransferases, like phosphoserine phosphatase, where the active site rearrangements in the equivalent domain are much smaller and not linked to cation binding at distant transport sites. The present observations, showing that in the Ca^{2+}-ATPase the close interaction of Gly^{626} and Asp^{703} with MgATP depends on Ca^{2+} binding at the transport sites, demonstrate an important difference from phosphoserine phosphatase, which may be fundamental to linking ion binding to phosphoryl transfer in the transport ATPases.

Acknowledgments—We thank Irene Mardarowicz and Joy Norman (University of Cape Town, Cape Town, South Africa) and Lene Jacobsen and Karin Kracht (University of Aarhus, Aarhus, Denmark) for expert technical assistance. We are indebted to Chikashi Toyoshima (University of Tokyo, Tokyo, Japan) for generously sharing information on unpublished work.

REFERENCES

1. Toyoshima, C., Nakasako, M., Nomura, H., and Ogawa, H. (2000) *Nature* **405,** 647–655
2. Toyoshima, C., and Nomura, H. (2002) *Nature* **418,** 605–611
3. McIntosh, D. B. (1998) *Adv. Mol. Cell. Biol.* **23A,** 33–99
4. Aravind, L., Galperin, M. Y., and Koonin, E. V. (1998) *Trends Biochem. Sci.* **23,** 127–129
5. Wang, W., Cho, H. S., Kim, R., Jancarik, J., Yokota, H., Nguyen, H. H., Grigoriev, I. V., Wemmer, D. E., and Kim, S.-H. (2002) *J. Mol. Biol.* **319,** 421–431
6. McIntosh, D. B., Woolley, D. G., MacLennan, D. H., Vilsen, B., and Andersen, J. P. (1999) *J. Biol. Chem.* **274,** 25227–25236
7. Clausen, J. D., McIntosh, D. B., Woolley, D. G., and Andersen, J. P. (2001) *J. Biol. Chem.* **276,** 35741–35750
8. Clarke, D. M., Loo, T. W., and MacLennan, D. H. (1990) *J. Biol. Chem.* **265,** 22223–22227
9. Vilsen, B., Andersen, J. P., and MacLennan, D. H. (1991) *J. Biol. Chem.* **266,** 16157–16164
10. Maruyama, K., Clarke, D. M., Fujii, J., Inesi, G., Loo, T. W., and MacLennan, D. H. (1989) *J. Biol. Chem.* **264,** 13038–13042
11. Kaufman, R. J., Davies, M. V., Pathak, V. K., and Hershey, J. W. (1989) *Mol. Cell. Biol.* **9,** 946–958
12. Chen, C., and Okayama, H. (1987) *Mol. Cell. Biol.* **7,** 2745–2752
13. Maruyama, K., and MacLennan, D. H. (1988) *Proc. Natl. Acad. Sci. U. S. A.* **85,** 3314–3318
14. Sørensen, T. L., Dupont, Y., Vilsen, B., and Andersen, J. P. (2000) *J. Biol. Chem.* **275,** 5400–5408
15. Andersen, J. P., Vilsen, B., Leberer, E., and MacLennan, D. H. (1989) *J. Biol. Chem.* **264,** 21018–21023
16. McIntosh, D. B., Woolley, D. G., Vilsen, B., and Andersen, J. P. (1996) *J. Biol. Chem.* **271,** 25778–25789
17. Dunaway-Mariano, D., and Cleland, W. W. (1980) *Biochemistry* **19,** 1496–1505
18. Hilge, M., Siegal, G., Vuister, G. W., Guntert, P., Gloor, S. M., and Abrahams, J. P. (2003) *Nat. Struct. Biol.* **10,** 468–474
19. McIntosh, D. B., and Woolley, D. G. (1994) *J. Biol. Chem.* **269,** 21587–21595
20. Clausen, J. D., McIntosh, D. B., Vilsen, B., Woolley, D. G., and Andersen, J. P. (2003) *J. Biol. Chem.* **278,** 20245–20258
21. Serpersu, E. H., Kirch, U., and Schoner, W. (1982) *Eur. J. Biochem.* **122,** 347–354
22. Vilsen, B, and Andersen, J. P. (1992) *J. Biol. Chem.* **267,** 3539–3550
23. McIntosh, D. B. (1992) *J. Biol. Chem.* **267,** 22328–22335
24. Lee, S.-Y., Cho, H. S., Pelton, J. G., Yan, D., Berry, E. A., and Wemmer, D. E. (2001) *J. Biol. Chem.* **276,** 16425–16431
25. Wakabayashi, S., and Shigekawa, M. (1987) *J. Biol. Chem.* **262,** 11524–11531

Roles of Conserved P Domain Residues and Mg^{2+} in ATP Binding in the Ground and Ca^{2+}-activated States of Sarcoplasmic Reticulum Ca^{2+}-ATPase

David B. McIntosh, Johannes D. Clausen, David G. Woolley, David H. MacLennan, Bente Vilsen and Jens Peter Andersen

J. Biol. Chem. 2004, 279:32515-32523.
doi: 10.1074/jbc.M403242200 originally published online May 7, 2004
